Sound scattering by anisotropic metafluids based on two-dimensional sonic crystals

Daniel Torrent and José Sánchez-Dehesa*

Department of Electronic Engineering, Wave Phenomena Group, Polytechnic University of Valencia, C/Camino de Vera sn, E-46022 Valencia, Spain

(Received 10 February 2009; revised manuscript received 31 March 2009; published 4 May 2009)

Multiple-scattering theory is here employed to study the scattering of sound by a fluidlike cylinder characterized by an anisotropic mass density tensor. A derivation of the t matrix associated to such acoustic material nonexisting in nature is here comprehensively derived, and the result is employed to study the pressure field produced by plane sound waves impinging the cylinder. It is also shown that an acoustic metamaterial or metafluid can be engineered to exactly match the dynamical properties of the anisotropic fluid by using a circular cluster made of a two-dimensional sonic crystal with a nonisotropic lattice.

DOI: 10.1103/PhysRevB.79.174104 PACS number(s): 62.65.+k, 43.20.+g

I. INTRODUCTION

Anisotropy is not a property of ordinary fluids. Anisotropy is a phenomenon commonly related with some kind of order and, in general, fluid materials are disordered structures. However, artificial fluids consisting of alternating layers of two different isotropic fluids were proposed by Shoenberg[1] in 1983. He predicted that this new type of fluid will behave, in the low-frequency limit, like an anisotropic acoustic material with a scalar bulk modulus but with dynamical mass density and sound speed as both anisotropic. He also derived the wave equation for the acoustic field in this anisotropic fluid, which do not exist in nature and is impossible to fabricate by usual means. The wave equation has been also derived by using a coordinate transformation approach.[2]

The interest in anisotropic fluids was recently boosted because of their possible applications such as media to control the flow of sound, in which being the acoustic cloaks is one the most exciting proposals.[3–9] The physical realization of anisotropic fluids can now be possible thanks to the recent advances in the field of sonic crystals (SCs), which are artificial structures made of sound scatterers periodically distributed in a fluid or gas background. SCs have been mainly studied from the 1990s because of their extraordinary properties for sound attenuation at wavelengths of the order of the lattice separation between scatterers. More recently, Cervera and co-workers[10] demonstrated that SC can be also used to build refractive acoustics devices, such as sonic lenses, for wavelengths large enough in comparison with the lattice separation between scatterers (homogenization limit). This result was supported later by numerical simulations based on different theoretical approaches.[11,12] Particularly, results obtained in the framework of multiple-scattering theory demonstrated that SC employed in Ref. 10 defines a new type of artificial isotropic fluids or metafluids whose acoustical parameters can be tailored with certain limitations.[12,13] Afterward, it was also predicted that the possibilities of tailoring for those metafluids even increase by combining sound scatterers of different elastic parameters in the SC.[14]

The possibility of obtaining anisotropic metafluids based on SC was first proposed by these authors[15] who also reported analytical formulas describing their anisotropic parameters, such as the dynamical mass density and sound speed, as a function of the scatterers filling fraction. More recently, we also made a proposal to engineer a two-dimensional (2D) acoustic cloak by using metafluids, with SC being the principal ingredient in its construction.[5]

In acoustics the scattering of sound by anisotropic scatterers is a topic scarcely treated in the literature for obvious reasons. This is not the case in optics, where the scattering of light by anisotropic scatterers is a phenomenon already studied[16–18] due to the fact that anisotropic dielectric materials are more common. Although anisotropy has been also studied for elastic waves in solids,[19,20] the scattering properties of anisotropic bodies is better known for the electromagnetic case.

In this paper we deeply analyzed the scattering properties of an anisotropic fluidlike circular cylinder, where the anisotropic parameters (density and speed of sound) are constant in Cartesian coordinates. These scattering properties are obtained by means of the t-matrix formalism.[21] Also, it is shown that a circular cylinder with such properties can be designed using the theory developed in Refs. 12–15, where it was demonstrated that SC in the homogenization limit (low-frequency regime) can be employed to build acoustic metamaterials or metafluids with desired dynamic properties. Finally, in order to verify the theory, the scattered field by circular cluster made of a 2D sonic crystal is calculated by the multiple-scattering method and show that, in fact, an anisotropic metafluid can be engineered by using SC.

The paper is organized as follows: in Sec. II the wave equation for anisotropic fluidlike materials is derived from the long-wavelength behavior of SC, and also the propagation of cylindrical waves in this medium are analyzed. Section III analyzes the scattering of waves by applying the boundary conditions and obtaining as a result the t matrix of the anisotropic cylinder. Section IV explains how to physically realize these types of anisotropic fluid by introducing metafluids based on SCs, and shows examples that could be engineered. The paper is summarized in Sec. V and hints on analytical derivations are given in the Appendix.

II. SOUND PROPAGATION IN ANISOTROPIC ACOUSTIC MEDIA

A. Wave equation

The wave equation describing the propagation of sound waves in anisotropic acoustic media can be obtained by using a phenomenological argument as follows. Let us assume that the anisotropic medium is made by placing sound scatterers in a nonisotropic periodic lattice and let us also assume that we work with wavelengths much larger than the lattice parameter. For example, it has been shown that 2D structured lattices of solid cylinders periodically arranged in lattices other than square or hexagonal behave like effective anisotropic fluids in the long-wavelength limit.[15] Under these assumptions, both the bulk modulus B and the density ρ are periodic functions of the spatial coordinates.

The linear acoustic equations for an inhomogeneous medium are[22]

$$\nabla P(\boldsymbol{r},t) + \rho(\boldsymbol{r})\frac{\partial \boldsymbol{V}(\boldsymbol{r},t)}{\partial t} = 0, \tag{1a}$$

$$\frac{\partial P(\boldsymbol{r},t)}{\partial t} + B(\boldsymbol{r})\,\nabla\cdot\boldsymbol{V}(\boldsymbol{r},t) = 0, \tag{1b}$$

where P describes the pressure field and $\boldsymbol{V}$ is the velocity vector field.

Now, let us consider that both $B(\boldsymbol{r})$ and $\rho(\boldsymbol{r})$ are periodic functions of the vector position $\mathbf{r}$. The goal is to find the form of the equations above in the low-frequency limit; that is, for the case in which the spatial periodicity defined by the wavelength is larger than the periodicity of the acoustic parameters B and ρ.

Therefore, plane-wave-like solutions can be proposed for both P and $\boldsymbol{V}$:

$$\begin{pmatrix} P(\boldsymbol{r},t) \\ \boldsymbol{V}(\boldsymbol{r},t)\end{pmatrix} = \begin{pmatrix} P(\boldsymbol{k},\omega) \\ \boldsymbol{V}(\boldsymbol{k},\omega)\end{pmatrix} e^{i\boldsymbol{k}\cdot\boldsymbol{r}}e^{-i\omega t}, \tag{2}$$

where the wave number is a function of the spatial coordinates, $\boldsymbol{k}=\boldsymbol{k}(\boldsymbol{r})$. Note that for low frequencies the spatial dependence of $\boldsymbol{k}$ disappears and the solutions become ordinary plane waves.

The spatial derivatives of functions in Eq. (2) are

$$\frac{\partial}{\partial x_i}\begin{pmatrix} P(\boldsymbol{r},t) \\ \boldsymbol{V}(\boldsymbol{r},t)\end{pmatrix} = i\begin{pmatrix} P(\boldsymbol{r},t) \\ \boldsymbol{V}(\boldsymbol{r},t)\end{pmatrix}\sum_j \chi_{ij}(\boldsymbol{r})k_j(\boldsymbol{r}), \tag{3}$$

where the tensorial quantity χ_{ij} is defined by

$$\chi_{ij}(\boldsymbol{r}) \equiv \delta_{ij} + \frac{x_j}{k_j(\boldsymbol{r})}\frac{\partial k_j(\boldsymbol{r})}{\partial x_i}. \tag{4}$$

In the low-frequency limit, this quantity is finite and different from zero and, as it is shown later, it is responsible for the anisotropy.

With these definitions Eqs. (1) become

$$iP(\boldsymbol{r},t)\sum_l \chi_{kl}(\boldsymbol{r})k_l(\boldsymbol{r}) + \rho(\boldsymbol{r})\frac{\partial V_k(\boldsymbol{r},t)}{\partial t} = 0, \tag{5a}$$

$$\frac{\partial P(\boldsymbol{r},t)}{\partial t} + iB(\boldsymbol{r})\sum_k\sum_j \chi_{kj}(\boldsymbol{r})k_j(\boldsymbol{r})V_k(\boldsymbol{r},t) = 0. \tag{5b}$$

Last equation can be simplified by defining an "effective particle velocity"

$$V_j^*(\boldsymbol{r},t) \equiv \sum_k \chi_{kj}(\boldsymbol{r})V_k(\boldsymbol{r},t), \tag{6}$$

yielding

$$\frac{\partial P(\boldsymbol{r},t)}{\partial t} + iB(\boldsymbol{r})\sum_j k_j(\boldsymbol{r})V_j^*(\boldsymbol{r},t) = 0. \tag{7}$$

This equation is suitable for averaging over the unit cell defined by the periodic system but not in its present form. For large wavelengths (homogenization limit) the pressure field and wave number are expected to be constant in the unit cell. But the effective particle velocity has an unknown behavior due to the quantities χ_{ij}, whose dependence in the spatial coordinates is unknown. Therefore, it is convenient to divide first by the bulk modulus B, and after that take the averaging,

$$\left\langle \frac{1}{B(\boldsymbol{r})}\right\rangle \frac{\partial P(\boldsymbol{r},t)}{\partial t} + i\sum_j k_j\langle V_j^*(\boldsymbol{r},t)\rangle = 0, \tag{8}$$

where it has been assumed that in the homogenization limit k is also constant. Since the bulk modulus does not interact with the periodicity of the lattice, the averaging can be easily performed.

For the case of a single scatterer per unit cell

$$\left\langle \frac{1}{B(\boldsymbol{r})}\right\rangle = \frac{1}{V_d}\int_{\text{cell}} \frac{1}{B(\boldsymbol{r})}dV = \frac{f}{B_a} + \frac{1-f}{B_b}, \tag{9}$$

where B_a and B_b are the bulk modulus of scatterer and background, respectively. Quantity f defines the filling fraction of the scatterer; i.e., the area of the scatterer divided by the area of the cell. This result is independent of the dimensionality of the problem and it is also independent of the scatterer's shape.

Defining the effective bulk modulus B^* as

$$\frac{1}{B^*} \equiv \left\langle \frac{1}{B(\boldsymbol{r})}\right\rangle = \frac{f}{B_a} + \frac{1-f}{B_b}, \tag{10}$$

and the cell-averaged particle velocity as

$$v_j^*(\boldsymbol{r},t) \equiv \langle V_j^*(\boldsymbol{r},t)\rangle, \tag{11}$$

the final form of Eq. (1) is

$$\frac{1}{B^*}\frac{\partial P(\boldsymbol{r},t)}{\partial t} + i\sum_j k_j v_j^*(\boldsymbol{r},t) = 0,$$

or

$$\frac{1}{B^*}\frac{\partial P(\boldsymbol{r},t)}{\partial t} + \nabla \cdot \boldsymbol{v}^*(\boldsymbol{r},t) = 0, \tag{12}$$

which has the same form as Eq. (1) but with a constant bulk modulus. Now it is also similar to the equation for a homogeneous medium.

This procedure can be also applied to Eq. (5) but working with V_j^* instead. After multiplying by χ_{kj} and adding for all k,

$$iP(\boldsymbol{r},t)\sum_l \sum_k \chi_{kj}(\boldsymbol{r})\chi_{kl}(\boldsymbol{r})k_l(\boldsymbol{r}) + \rho(\boldsymbol{r})\frac{\partial V_j^*(\boldsymbol{r},t)}{\partial t} = 0. \tag{13}$$

This equation cannot be averaged because of the product between $\rho(\boldsymbol{r})$ and the temporal derivative of $V_j^*(\boldsymbol{r},t)$. We divide first by the density and, after averaging, we get

$$iP(\boldsymbol{r},t)\sum_\ell \rho_{j\ell}^{*-1}k_\ell + \frac{\partial v_j^*(\boldsymbol{r},t)}{\partial t} = 0, \tag{14}$$

where $\rho_{j\ell}^{*-1}$ are defined as

$$\rho_{j\ell}^{*-1} \equiv \left\langle \rho^{-1}(\boldsymbol{r})\sum_k \chi_{kj}(\boldsymbol{r})\chi_{k\ell}(\boldsymbol{r})\right\rangle. \tag{15}$$

These are the matrix elements of the reciprocal of the effective-mass density tensor; i.e., $\Sigma_\ell \rho_{j\ell}^{*-1}\rho_{\ell i}^* = \delta_{ji}$.

Therefore, Eq. (14) can also be cast into

$$ik_\ell P(\boldsymbol{r},t) + \sum_j \rho_{\ell j}^*\frac{\partial v_j^*(\boldsymbol{r},t)}{\partial t} = 0. \tag{16}$$

In vectorial differential form

$$\nabla P(\boldsymbol{r},t) + \boldsymbol{\rho}^* : \frac{\partial \boldsymbol{v}^*(\boldsymbol{r},t)}{\partial t} = 0. \tag{17}$$

By solving for the pressure field we arrive to the wave equation

$$\sum_{i,k}\rho_{ik}^{*-1}\frac{\partial^2 P}{\partial x_k\,\partial x_i} - \frac{1}{B^*}\frac{\partial^2 P}{\partial t^2} = 0, \tag{18}$$

which is obviously anisotropic due to the presence of the cross terms in the partial derivatives.

By trying plane-wave solutions of the form

$$P(\boldsymbol{r},t) = P(\boldsymbol{k},\omega)e^{i\boldsymbol{k}\cdot\boldsymbol{r}}e^{-i\omega t}, \tag{19}$$

the relationship between the frequency and the wave number is finally obtained:

$$\omega^2 = k^2 B^* \sum_{i,k}\rho_{ki}^{*-1}\cos\tau_i \cos\tau_k, \tag{20}$$

where the wave vector components have been assumed with the form $k_i = k\cos\tau_i$.

Expression (20) lets us conclude that the relation between the effective sound speed tensor c_{ki}^* and the reciprocal of the mass density tensor ρ_{ki}^{*-1} is similar to that for the isotropic case[23]

$$c_{ki}^{*2} = B^*\rho_{ki}^{*-1}. \tag{21}$$

In the rest of the paper asterisks will be omitted for simplification purposes unless it is specifically indicated.

B. Cylindrical waves in anisotropic fluidlike materials

The spatial part of an anisotropic plane wave is

$$P(\boldsymbol{r}) = P(\boldsymbol{k})e^{i\boldsymbol{k}\cdot\boldsymbol{r}}. \tag{22}$$

If there is no z dependence of P, the problem reduces to a 2D problem in the XY plane, where the wave vector $\boldsymbol{k} = k(\tau)(\cos\tau, \sin\tau)$ with $k(\tau) = \omega/c(\tau)$ defines a wave front whose direction of propagation makes an angle τ with the x axis.

In this work only nondivergent fields are considered and, therefore, only real angles τ are considered in the integration above. As a consequence the quantity $P(\boldsymbol{k}) = P(\omega,\tau)$ can be Fourier expanded

$$P(\omega,\tau) = \frac{1}{2\pi}\sum_s i^{-s}B_s(\omega)e^{is\tau}. \tag{23}$$

By inserting this expansion into Eq. (22) and after integration over all τ angles, a general pressure wave is obtained

$$P(\boldsymbol{r}) = \sum_s B_s(\omega)\frac{i^{-s}}{2\pi}\int_{-\pi}^{\pi} e^{i\boldsymbol{k}\cdot\boldsymbol{r}}e^{is\tau}d\tau. \tag{24}$$

This expansion is equivalent to

$$P(U) = \sum_s B_s J_s^a(\omega r/c,\theta)e^{is\theta}, \tag{25}$$

where the anisotropic cylindrical function J_s^a has been defined as

$$J_s^a(\omega r/c,\theta) \equiv \frac{i^{-s}}{2\pi}\int_{-\pi}^{\pi} e^{i\boldsymbol{k}\cdot\boldsymbol{r}}e^{is(\tau-\theta)}d\tau. \tag{26}$$

Notice that for an isotropic medium the function J_s^a reduces to the Bessel function of order s.[24]

III. SCATTERING OF SOUND WAVES BY AN ANISOTROPIC FLUIDLIKE CYLINDER

A. Boundary conditions

Boundary conditions at the interface of two isotropic fluids are the continuity of the pressure field P and the normal component of the particle velocity field $\boldsymbol{v}$, respectively:

$$P^+ = P^-, \tag{27a}$$

$$\boldsymbol{n}\cdot\boldsymbol{v}^+ = \boldsymbol{n}\cdot\boldsymbol{v}^-, \tag{27b}$$

where $\boldsymbol{n}$ is the unitary vector normal to the boundary surface.

These conditions can be generalized for anisotropic fluidlike materials but the tensorial nature of the dynamical mass density tensor should be taken into account.

From Eq. (17) in stationary form the particle velocity field is

$$\boldsymbol{v} = -\frac{i\boldsymbol{\rho}^{-1}}{\omega}\nabla P, \tag{28}$$

where the reciprocal of the dynamical mass density $\boldsymbol{\rho}^{-1}$ is a tensor and, then, the normal component of the particle velocity is

$$\boldsymbol{n}\cdot\boldsymbol{v} = -\boldsymbol{n}\cdot\frac{i\boldsymbol{\rho}^{-1}}{\omega}\boldsymbol{\nabla}P = -\frac{i}{\omega}\sum_{k,l} n_k\rho_{kl}^{-1}\frac{\partial P}{\partial x_l}. \qquad (29)$$

In polar coordinates:

$$\boldsymbol{n}\cdot\boldsymbol{v} = -\frac{i}{\omega}\left[\rho_{rr}^{-1}(\theta)\frac{\partial P}{\partial r} + \frac{1}{r}\rho_{r\theta}^{-1}(\theta)\frac{\partial P}{\partial \theta}\right], \qquad (30)$$

in which

$$\rho_{rr}^{-1}(\theta) = \rho_{s+}^{-1} + \rho_{s-}^{-1}\cos 2\theta + \rho_{a+}^{-1}\sin 2\theta, \qquad (31a)$$

$$\rho_{r\theta}^{-1}(\theta) = -\rho_{s-}^{-1}\sin 2\theta + \rho_{a+}^{-1}\cos 2\theta, \qquad (31b)$$

and

$$\rho_{s\pm}^{-1} = \frac{\rho_{xx}^{-1} \pm \rho_{yy}^{-1}}{2}, \qquad (32a)$$

$$\rho_{a\pm}^{-1} = \frac{\rho_{xy}^{-1} \pm \rho_{yx}^{-1}}{2}. \qquad (32b)$$

From Eq. (15) it is deduced that $\rho_{xy}^{-1}=\rho_{yx}^{-1}$, and then

$$\rho_{a+}^{-1} = \rho_{xy}^{-1}, \qquad (33a)$$

$$\rho_{a-}^{-1} = 0. \qquad (33b)$$

Technical details of how to calculate the elements of matrix density are given in Ref. 15.

B. *t* matrix of an anisotropic fluidlike cylinder

Let us consider a cylinder of radius R, anisotropic mass density ρ_{ij}, and bulk modulus B_a. It is embedded in a homogeneous isotropic fluid of acoustic parameters ρ_b and B_b. When some arbitrary incident field P^0, given by

$$P^0(r,\theta;\omega) = \sum_q A_q^0 J_q(\omega/c_b r)e^{iq\theta}, \qquad (34)$$

impinges the cylinder, a scattered field $P^{\rm sc}$ is excited,

$$P^{\rm sc}(r,\theta;\omega) = \sum_q A_q H_q(\omega/c_b r)e^{iq\theta}, \qquad (35)$$

where H_q are the Hankel functions.

This section is devoted to obtaining the t matrix that relates coefficients A_q and A_q^0,[21]

$$A_q = \sum_s T_{qs}A_s^0, \qquad (36)$$

where coefficients T_{qs} define the t matrix elements.

Section I demonstrated that sound waves traveling inside an anisotropic fluid propagate with a speed that is angle dependent,

$$c^2(\tau) = \sum_{i,j} c_{ij}^2 \cos\tau_i \cos\tau_j, \qquad (37)$$

where tensor c_{ij} already appeared in Eq. (21).

For positions outside the cylinder, $r>R$, the total field P is obtained by adding the incident and scattered fields:

$$P(r,\theta;\omega) = \sum_s A_s^0 J_s(k_b r)e^{is\theta} + \sum_s A_s H_s(k_b r)e^{is\theta}, \qquad (38)$$

with k_b as the wave vector in the propagating medium $k_b=\omega/c_b$.

Inside the cylinder, $r\le R$, the proposed solution for wave propagation inside the cylinder is a linear combination of plane waves of the form

$$P(r,\theta;\omega) = \sum_s B_s J_s^a(kr,\theta)e^{is\theta}, \qquad (39)$$

where

$$J_s^a(kr,\theta) = \frac{i^{-s}}{2\pi}\int_{-\pi}^{\pi}\exp\{i[\omega r/c(\tau)]\cos(\tau-\theta)\}e^{is(\tau-\theta)}d\tau, \qquad (40)$$

and k is the wave vector inside the cylinder, $k=\omega/c(\tau)$. Note that the anisotropy is embedded in k.

Integral is performed for all the angles τ real, excluding angles with imaginary part. Evanescent modes are excluded because we are only interested in the field inside the cylinder with no sources. If we were interested in scattered fields in the anisotropic medium, the evanescent modes should be taken into account.

Boundary conditions in Eqs. (27a) and (27b) become

$$\sum_s A_s^0 J_s(k_b R)e^{is\theta} + \sum_s A_s H_s(k_b R)e^{is\theta} = \sum_s B_s J_s^a(\omega R/c,\theta)e^{is\theta}, \qquad (41a)$$

$$\frac{k_b}{\rho_b}\frac{\partial}{\partial(k_b r)}\left[\sum_s A_s^0 J_s(k_b r)e^{is\theta} + \sum_s A_s H_s(k_b r)e^{is\theta}\right]_{r=R} = \sum_s B_s v_r^s, \qquad (41b)$$

where

$$v_r^s = \left[\rho_{rr}^{-1}(\theta)\frac{\partial}{\partial r} + \frac{1}{r}\rho_{r\theta}^{-1}(\theta)\frac{\partial}{\partial\theta}\right]_{r=R} J_s^a(\omega r/c,\theta)e^{is\theta}.$$

Radial functions on the right side of both equations are coupled with the angular variable θ. Now it is not possible to just cancel the factors $e^{iq\theta}$. After multiplying both equations by $\frac{1}{2\pi}e^{-iq\theta}$ and integrating from $-\pi$ to π,

$$A_q^0 J_q(k_b R) + A_q H_q(k_b R) = \sum_s N_{qs}B_s, \qquad (42a)$$

$$A_q^0 J_q'(k_b R) + A_q H_q'(k_b R) = \sum_s M_{qs}B_s, \qquad (42b)$$

where the $'$ implies derivation with respect to the argument and

$$N_{qs} = \frac{1}{2\pi}\int_{-\pi}^{\pi} J_s^a(\omega R/c,\theta)e^{i(s-q)\theta}d\theta, \qquad (43a)$$

$$M_{qs} = \frac{\rho_b}{2k_b\pi}\int_{-\pi}^{\pi}\left[\rho_{rr}^{-1}(\theta)\frac{\partial}{\partial r} + \frac{1}{r}\rho_{r\theta}^{-1}(\theta)\frac{\partial}{\partial\theta}\right]_{r=R} \times [J_s^a(\omega r/c,\theta)e^{is\theta}]e^{-iq\theta}d\theta. \quad (43b)$$

Technical details of how to calculate these matrix elements are given in Appendix.

By using the relationship

$$J_q(k_br)H_q'(k_br) - J_q'(k_br)H_q(k_br) = \frac{2i}{\pi k_br}, \quad (44)$$

together with Eqs. (43a) and (43b) the following relations are obtained

$$A_q^0 = -\frac{i\pi k_bR}{2}\sum_s [H_q'(k_bR)N_{qs} - H_q(k_bR)M_{qs}]B_s, \quad (45)$$

$$A_q = \frac{i\pi k_bR}{2}\sum_s [J_q'(k_bR)N_{qs} - J_q(k_bR)M_{qs}]B_s. \quad (46)$$

By defining the matrices

$$H_{qs} \equiv \frac{i\pi k_bR}{2}[H_q'(k_bR)N_{qs} - H_q(k_bR)M_{qs}], \quad (47a)$$

$$J_{qs} \equiv \frac{i\pi k_bR}{2}[J_q'(k_bR)N_{qs} - J_q(k_bR)M_{qs}]. \quad (47b)$$

Equations above can be cast in a matrix form,

$$\boldsymbol{A}^0 = -\boldsymbol{HB}, \quad (48)$$

$$\boldsymbol{A} = \boldsymbol{JB}, \quad (49)$$

$$\boldsymbol{A} = -\boldsymbol{JH}^{-1}\boldsymbol{A}^0, \quad (50)$$

so that the t matrix of the cylinder is given by

$$\boldsymbol{T} = -\boldsymbol{JH}^{-1}. \quad (51)$$

As a numerical application of this t matrix we have considered the case of an anisotropic cylinder with parameters $B_a = 1.36B_b$, $\rho_{xx}=1.52\rho_b$, and $\rho_{yy}=2.2\rho_b$. The amplitude of the total pressure along the x direction, $|P(r,\theta=0)|$, is obtained from Eqs. (38) and (39). Figure 1 plots the results for different orientations of the cylinder with respect to the x axis. The results are obtained by considering an incident sound plane wave with $\lambda=R/2$. It is clearly shown that the scattering properties of the cylinder effectively depend on its orientation with respect to the excited sound that is kept constant.

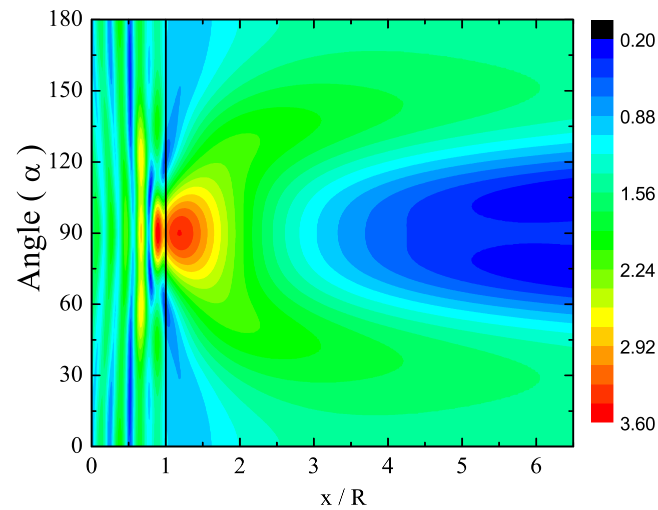

FIG. 1. (Color online) Amplitude of the total pressure produced by an incident sound plane wave impinging from the left over an anisotropic cylinder of radius R placed at the origin of coordinates. The pressure is represented along the x axis in normalized units. The vertical axis represents the rotation angle α of the cylinder with respect to the x axis. The wavelength of the incident field is $\lambda = R/2$. The black dashed line defines the border of cylinder.

IV. PHYSICAL REALIZATION: METAFLUIDS BASED ON SONIC CRYSTALS

Section II demonstrated that a periodic arrangement of sound scatterers can lead to anisotropic fluidlike behavior. Moreover, analytical expressions for the effective acoustic parameters of anisotropic metafluids based on 2D arrays of elastic cylinders were already reported by these authors.[15] Therefore, it is expected that, when an infinite periodic system is cut with a circular shape, the resulting cluster of cylinders should behave in the low-frequency limit such as an anisotropic fluidlike cylinder with the same dynamical properties than that of the infinite medium.

In previous works the authors analyzed finite-size effects such as ordering/disordering in the cluster[12,13] or the dependence of the effective parameters as a function of the cluster size.[25] It was demonstrated that, for isotropic lattices, the acoustic parameters of the cluster are the same as that of the infinite medium when the cluster is large enough. Now it is shown below that the same property is also accomplished for the case of anisotropic lattices.

As an example let us consider the case of a 2D lattice of rigid cylinders in which the lattice vectors a_1 and a_2 form an angle $\Phi=75°$, and the ratio between their moduli is $b/a=2$, that is,

$$\boldsymbol{a}_1 = a\hat{x}, \quad (52a)$$

$$\boldsymbol{a}_2 = b\cos\Phi\hat{x} + b\sin\Phi\hat{y} \approx 0.52a\hat{x} + 1.93a\hat{y}. \quad (52b)$$

The filling fraction of this lattice is $f=\pi R^2/(ab\sin\Phi) = (\pi/2\sin\Phi)(R/a)^2$, where R is the cylinder's radius. The condition of maximum packing (closed packing) is achieved for $R=0.5a$ that implies $f_{CP}=0.406$. The assumption of rigid cylinders (i.e., infinite mass) is taken for numerical simplifications

Figure 2 shows the behavior of the effective acoustic parameters for this anisotropic 2D lattice (see the inset) of rigid cylinders in a homogeneous isotropic fluid of parameter B_b and ρ_b as a function of its filling fraction. It is observed that the resulting metafluid obtained by using that anisotropic lattice is also anisotropic because of the different values taken by magnitudes such as ρ_{xx} and ρ_{yy} for the same f. Note that c_{ij}^* and ρ_{ij}^* are related through Eq. (21). Therefore, it is

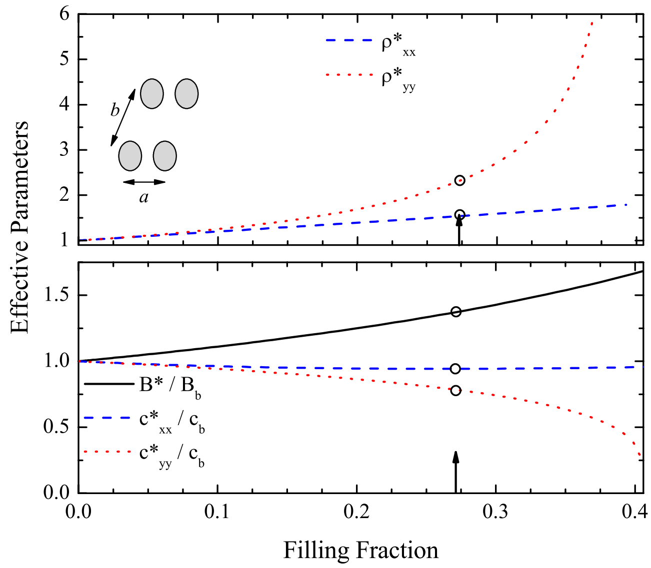

FIG. 2. (Color online) Effective parameters of a 2D sonic crystal of rigid cylinders as a function of the lattice filling fraction. The lattice vectors make an angle of $\Phi=75°$ and the ratio of their modulus is $b/a=2$.

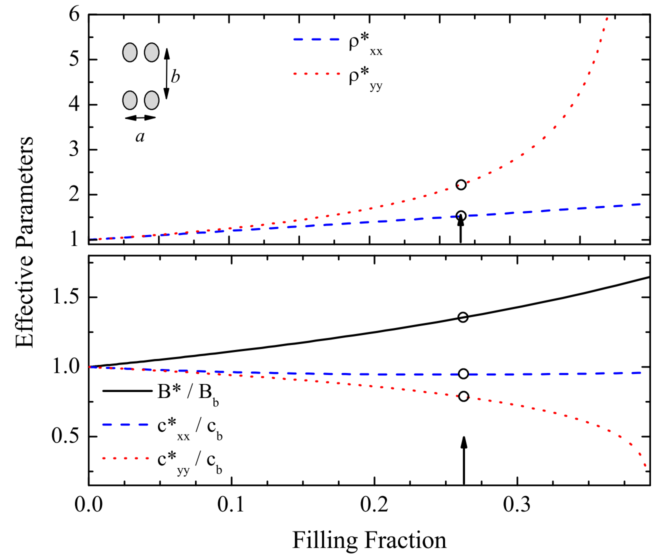

FIG. 4. (Color online) Effective parameters of a two-dimensional sonic crystal of rigid cylinders as a function of the lattice filling fraction. The lattice vectors make an angle of $\Phi=90°$ and the ratio of their modulus is $b/a=2$.

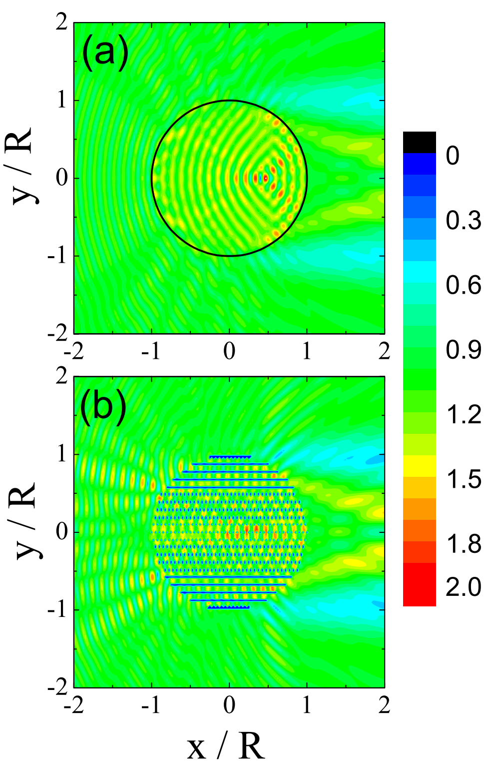

FIG. 3. (Color online) (a) Pressure scattered by an anisotropic fluidlike cylinder for an impinging plane wave propagating along the x axis such that $kR=8\pi$, and with acoustic parameters. (b) Multiple scattering simulation for the same plane wave impinging over a cluster of rigid cylinders of radius $R_0=0.41a$ embedded in the two-dimensional lattice described in Fig. 2. The wavelength of the field also satisfies $kR_{\rm eff}\approx 8\pi$. The effective parameters for this filling fraction are the same as that of the anisotropic cylinder in (a).

expected that a finite cluster (of circular shape) based on this SC will behave dynamically as an anisotropic fluidlike cylinder with the same acoustic parameters than that obtained for the infinite lattice (see Fig. 2).

To verify the last conclusion we simulate the scattering properties of an anisotropic fluid cylinder with parameters $B_a=1.374B_b$, $\rho_{xx}^{-1}=0.649\rho_b^{-1}$, and $\rho_{yy}^{-1}=0.424\rho_b^{-1}$ in order to compare them with that of a metafluid based on SC with the same anisotropic parameters. The vertical arrow in Fig. 2 defines the filling fraction of the lattice producing a metafluid with the same anisotropic parameters (symbols) as that of the homogeneous anisotropic cylinder.

Figure 3 shows a comparison between both field distributions near (and inside) an anisotropic fluidlike cylinder [see Fig. 3(a)] and the corresponding metafluid made of 657 rigid cylinders [see Fig. 3(b)]. As incident field we have considered a sound plane-wave incident from the left, with $\lambda=R/4\approx R_{\rm eff}/4$, where R and $R_{\rm eff}$ are the radii of cylinder and cluster, respectively. For the case of the anisotropic fluid cylinder, the field distribution has been obtained by using the t matrix described in Sec. III. For the cluster the map field was obtained by the multiple-scattering method.[12,13] It can be shown how both field distributions are practically the same even at the interior of the circle. However, additional diffraction effects appear for the case of the cluster metafluid. Let us point out that the working wavelength in terms of the lattice parameter is $\lambda=5a$. Therefore the homogenization condition established in our previous work[12] is accomplished, i.e., $\lambda\geq 4a$.

For the sake of its comparison, we have also studied the case of a rectangular lattice, i.e., when $\Phi=90°$ and $b=2a$. Figure 4 depicts the behavior of the acoustic parameters for this new metafluid. The behavior is slightly different to that of the previous case because there is only a small variation in the geometry in the new anisotropic 2D lattice (see inset).

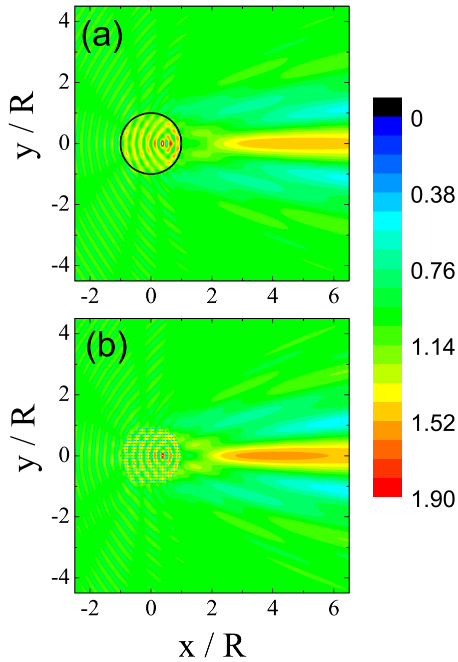

FIG. 5. (Color online) (a) Map of the total field scattered by an anisotropic fluidlike cylinder. The impinging sound wave propagates along the x axis with $kR=4\pi$. (b) Multiple scattering simulation for the total field scattered by the metafluid made of a cluster of 657 rigid cylinders arranged in the 2D lattice described in Fig. 4. The metafluid has the same parameters than in (a).

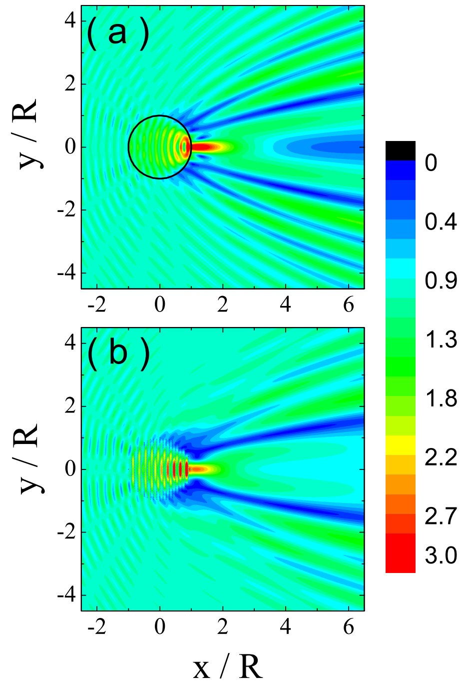

FIG. 6. (Color online) [(a) and (b)] Total pressure 2D maps calculated with same conditions as in Fig. 5 but now the cylinder and cluster are rotated 90°.

Now the close packing is achieved for $f_{\mathrm{CP}}=0.393$. As in the previous lattice, it can be shown how the component along x of the sound speed tensor changes slightly as a function of filling fraction while the y component suddenly drops to zero when the nearest neighbors cylinders along x touch. However, the magnitudes ρ_{xx}-ρ_{yy} are larger now for the same f. Therefore, this system represents a metafluid that is more anisotropic than that obtained by the nonrectangular lattice. Regarding the effective bulk modulus, note that its behavior as a function of filling fraction is similar to that in Fig. 2 because the lattice vectors in both cases have the same ratio b/a between moduli.

Figures 5 and 6 give 2D maps of total pressure field amplitudes obtained when a sound plane-wave incident from the negative x axis impinges the cylinder or the cluster. Figure 6 represent the cases in which the cylinder and the cluster are rotated 90° with respect to those represented in Fig. 5. The working wavelength is in this case twice than that used in Fig. 3, i.e., $\lambda=10a$, and the homogenization condition is also guaranteed. The selected parameters of the nonexisting anisotropic fluid cylinder are $B_a=1.357B_b$, $\rho_{xx}^{-1}=0.659\rho_b^{-1}$, and $\rho_{yy}^{-1}=0.455\rho_b^{-1}$. These parameters are obtained with a metafluid cluster made of 657 rigid cylinders arranged on a rectangular lattice with $f=0.263$ (see the arrows in Fig. 4). Note in Fig. 5 how the highly collimated beam observed in the far field when cylinder and cluster are both oriented along x becomes a shadow when both are rotated $\Phi=90°$. This is a demonstration of the strong anisotropic effects obtained by these types of lattices. Moreover, Fig. 6 shows that a strong focusing effect appears near the cylinder and cluster surfaces. This phenomenon is obtained because of incident wave encounters with the cylinder oriented along the direction in which the component of the mass density tensor is huge. These extraordinary properties could be used to design tunable acoustical devices based on these artificial acoustic structures named as metafluids.

V. SUMMARY

We have reported a comprehensive derivation of the t matrix for an anisotropic fluidlike cylinder. This formulation is of extraordinary interest for studying the recently introduced acoustic metamaterials or metafluids that, thanks to their anisotropic properties, makes possible development of exciting new acoustical devices such as acoustic cloaks.[3–9] Also, we have shown that anisotropic metafluids can be obtained by exploiting the homogenization properties of SC made of anisotropic lattices of rigid cylinders. Particularly, we have shown that the scattering properties of nonexisting anisotropic fluid cylinder can be exactly reproduced by metafluids based on SC.

ACKNOWLEDGMENTS

We acknowledge the financial support by the Spanish Ministerio de Ciencia e Innovación (MICIIN) under programs TEC (Ref. TEC2007-67239) and CONSOLIDER (Ref. CSD2008-66). D.T. acknowledges a grant also supported by MICIIN.

APPENDIX: NUMERICAL CALCULATION OF THE *t* MATRIX

The matrix elements N_{qs} and M_{qs} must be evaluated in numerical simulations. However their expressions in Eqs.

(43a) and (43b) are not appropriated for an easy computation because it requires a double integration that is very inefficient. This Appendix demonstrates that these elements can be expressed as integrals of Bessel functions.

1. Calculation of N_{qs}

By using the integral form of J_s^a the elements N_{qs} can be expressed as

$$N_{qs}=\frac{1}{2\pi}\int_{-\pi}^{\pi}d\theta\frac{i^{-s}}{2\pi}\int_{-\pi}^{\pi}\exp[i(\omega r/c)\cos(\tau-\theta)]\times e^{is(\tau-\theta)}d\tau e^{i(s-q)\theta}. \tag{A1}$$

If the integration is made first with respect to θ, reordering the terms, one finds

$$N_{qs}=\frac{i^{q-s}}{2\pi}\int_{-\pi}^{\pi}e^{i(s-q)\tau}d\tau\frac{i^{-q}}{2\pi}\int_{-\pi}^{\pi}\exp[i(\omega r/c)\cos(\theta-\tau)]d\theta\times e^{-iq(\theta-\tau)}. \tag{A2}$$

Note that, as c is function of τ and not of θ, the above equation is equivalent to

$$N_{qs}=\frac{i^{q-s}}{2\pi}\int_{-\pi}^{\pi}J_q(\omega r/c)e^{i(s-q)\tau}d\tau. \tag{A3}$$

2. Calculation of M_{qs}

These elements do not easily simplify because of the derivatives that have to be performed. It is convenient to split them into

$$M_{qs}=I_{qs}^{(r)}+I_{qs}^{(\theta)}, \tag{A4}$$

where

$$I_{qs}^{(r)}=\frac{\rho_b}{2k_b\pi}\int_{-\pi}^{\pi}\left[\rho_{rr}^{-1}(\theta)\frac{\partial}{\partial r}\right]_{r=R}[J_s^a(\omega r/c,\theta)e^{is\theta}]e^{-iq\theta}d\theta, \tag{A5}$$

$$I_{qs}^{(\theta)}=\frac{\rho_b}{2k_b\pi}\int_{-\pi}^{\pi}\left[\frac{1}{r}\rho_{r\theta}^{-1}(\theta)\frac{\partial}{\partial\theta}\right]_{r=R}[J_s^a(\omega r/c,\theta)e^{is\theta}]e^{-iq\theta}d\theta. \tag{A6}$$

Applying the differential operators and using the integral definition of $J_s^a e^{is\theta}$ given by Eq. (26), and reminding that $k_b=\omega/c_b$, it is found that

$$I_{qs}^{(r)}=\frac{i^{-s}}{(2\pi)^2}\int_{-\pi}^{\pi}\int_{-\pi}^{\pi}\frac{i\rho_b c_b}{c(\tau)}\rho_{rr}^{-1}\cos(\tau-\theta)\times\exp[i(\omega R/c)\cos(\tau-\theta)]e^{is\tau}e^{-iq\theta}d\theta d\tau, \tag{A7}$$

and

$$I_{qs}^{(\theta)}=\frac{i^{-s}}{(2\pi)^2}\int_{-\pi}^{\pi}\int_{-\pi}^{\pi}\frac{i\rho_b c_b}{c(\tau)}\rho_{r\theta}^{-1}\sin(\tau-\theta)\times\exp[i(\omega R/c)\cos(\tau-\theta)]e^{is\tau}e^{-iq\theta}d\theta d\tau. \tag{A8}$$

But, it can be shown that

$$\rho_{rr}^{-1}\cos(\tau-\theta)+\rho_{r\theta}^{-1}\sin(\tau-\theta)=\rho_{s+}^{-1}\cos(\tau-\theta)+\rho_{s-}^{-1}\cos(\tau+\theta)+\rho_{a+}^{-1}\sin(\tau+\theta), \tag{A9}$$

therefore, the sum of $I_{qs}^{(r)}$ and $I_{qs}^{(\theta)}$ and then M_{qs} can be expressed as a sum of the following three integrals

$$I_{qs}^{(1)}=\frac{i^{-s}}{(2\pi)^2}\rho_{s+}^{-1}\int_{-\pi}^{\pi}\int_{-\pi}^{\pi}\frac{i\rho_b c_b}{c}\cos(\tau-\theta)\times\exp[i(\omega R/c)\cos(\tau-\theta)]e^{is\tau}e^{-iq\theta}d\theta d\tau, \tag{A10}$$

$$I_{qs}^{(2)}=\frac{i^{-s}}{(2\pi)^2}\rho_{s-}^{-1}\int_{-\pi}^{\pi}\int_{-\pi}^{\pi}\frac{i\rho_b c_b}{c}\cos(\tau+\theta)\times\exp[i(\omega R/c)\cos(\tau-\theta)]e^{is\tau}e^{-iq\theta}d\theta d\tau, \tag{A11}$$

$$I_{qs}^{(3)}=\frac{i^{-s}}{(2\pi)^2}\rho_{a+}^{-1}\int_{-\pi}^{\pi}\int_{-\pi}^{\pi}\frac{i\rho_b c_b}{c}\sin(\tau+\theta)\times\exp[i(\omega R/c)\cos(\tau-\theta)]e^{is\tau}e^{-iq\theta}d\theta d\tau. \tag{A12}$$

Defining

$$\mathrm{SC}_p(x)=\frac{1}{2i^p}[e^{ix}+(-1)^p e^{-ix}];p=0,1, \tag{A13}$$

the integral,

$$\int_{-\pi}^{\pi}\mathrm{SC}_p(\tau\pm\theta)\exp[i(\omega R_0/c)\cos(\tau-\theta)]e^{iq(\tau-\theta)}d\theta, \tag{A14}$$

can be expressed as a function of Bessel functions

$$\frac{2\pi i^{q\pm1}}{2i^p}[e^{i(\alpha\pm\alpha)}J_{q\pm1}(\omega R_0/c)-(-1)^p e^{-i(\alpha\pm\alpha)}J_{q\mp1}(\omega R_0/c)], \tag{A15}$$

then the three integrals become

$$I_{qs}^{(1)}=\frac{i^{-(s-q)}}{2\pi}\rho_b\rho_{s+}^{-1}\int_{-\pi}^{\pi}\frac{c_b}{c}\frac{1}{2}[J_{q-1}(\omega R/c)-J_{q+1}(\omega R/c)]e^{i(s-q)\tau}d\tau, \tag{A16a}$$

$$I_{qs}^{(2)}=\frac{i^{-(s-q)}}{2\pi}\rho_b\rho_{s-}^{-1}\int_{-\pi}^{\pi}\frac{c_b}{c}\frac{1}{2}[e^{-2i\tau}J_{q-1}(\omega R_0/c)-e^{2i\tau}J_{q+1}(\omega R_0/c)]e^{i(s-q)\tau}d\tau, \tag{A16b}$$

$$I_{qs}^{(3)}=\frac{i^{-(s-q)}}{2\pi}\rho_b\rho_{a+}^{-1}\int_{-\pi}^{\pi}\frac{c_b}{c}\frac{i}{2}[e^{2i\tau}J_{q+1}(\omega R_0/c)+e^{-2i\tau}J_{q-1}(\omega R_0/c)]e^{i(s-q)\tau}d\tau. \tag{A16c}$$

By adding the three terms, we arrive at

$$M_{qs} = \frac{i^{-(s-q)}}{2\pi} \int_{-\pi}^{\pi} \frac{c_b}{c} e^{i(s-q)\tau} d\tau \left[\rho_b \rho_{rr}^{-1}(\tau) \frac{\partial J_q(\omega R/c)}{\partial(\omega R/c)} + i \rho_b \rho_{r\tau}^{-1}(\tau + \pi/2) \frac{qc}{\omega R} J_q(\omega R/c) \right]. \tag{A17}$$

This expression is more appropriate for numerical computations.

*jsdehesa@upvnet.upv.es

[1] M. Schoenberg, J. Acoust. Soc. Am. **73**, 61 (1983).
[2] G. Milton, M. Briane, and J. Willis, New J. Phys. **8**, 248 (2006).
[3] S. Cummer and D. Schurig, New J. Phys. **9**, 45 (2007).
[4] L.-W. Cai and J. Sanchez-Dehesa, New J. Phys. **9**, 450 (2007).
[5] D. Torrent and J. Sánchez-Dehesa, New J. Phys. **10**, 063015 (2008).
[6] Y. Cheng, F. Yang, J. Y. Xu, and X. J. Liu, Appl. Phys. Lett. **92**, 151913 (2008).
[7] S. A. Cummer, B. I. Popa, D. Schurig, D. R. Smith, J. Pendry, M. Rahm, and A. Starr, Phys. Rev. Lett. **100**, 024301 (2008).
[8] H. Chen and C. Chan, Appl. Phys. Lett. **91**, 183518 (2007).
[9] A. N. Norris, Proc. R. Soc. London, Ser. A **464**, 2411 (2008).
[10] F. Cervera, L. Sanchis, J. V. Sánchez-Pérez, R. Martinez-Sala, C. Rubio, F. Meseguer, C. López, D. Caballero, and J. Sánchez-Dehesa, Phys. Rev. Lett. **88**, 023902 (2001).
[11] A. A. Krokhin, J. Arriaga, and L. N. Gumen, Phys. Rev. Lett. **91**, 264302 (2003).
[12] D. Torrent, A. Hakansson, F. Cervera, and J. Sanchez-Dehesa, Phys. Rev. Lett. **96**, 204302 (2006).
[13] D. Torrent and J. Sánchez-Dehesa, Phys. Rev. B **74**, 224305 (2006).
[14] D. Torrent and J. Sánchez-Dehesa, New J. Phys. **9**, 323 (2007).
[15] D. Torrent and J. Sánchez-Dehesa, New J. Phys. **10**, 023004 (2008).
[16] J. C. Monzon and N. J. Damaskos, IEEE Trans. Antennas Propag. **34**, 1243 (1986).
[17] J. C. Monzon, IEEE Trans. Antennas Propag. **35**, 670 (1987).
[18] X. B. Wu and K. Yasumoto, J. Appl. Phys. **82**, 1996 (1997).
[19] M. Musgrave, Rep. Prog. Phys. **22**, 74 (1959).
[20] P. C. Waterman, Phys. Rev. **113**, 1240 (1959).
[21] P. C. Waterman, J. Acoust. Soc. Am. **45**, 1417 (1969).
[22] P. G. Bergmann, J. Acoust. Soc. Am. **17**, 329 (1946).
[23] A. Wood, *A Textbook of Sound* (MacMillan, New York, 1941).
[24] I. A. Milton Abramowitz, *Handbook of Mathematical Functions* (Dover, New York, 1972).
[25] D. Torrent, J. Sanchez-Dehesa, and F. Cervera, Phys. Rev. B **75**, 241404(R) (2007).